2018 IEEE Intelligent Vehicles Symposium (IV)
Changshu, Suzhou, China, June 26-30, 2018

A Fallback Approach for an Automated Vehicle Encountering Sensor Failure in Monitoring Environment

Wei Xue*, Bo Yang†, Tsutomu Kaizuka† and Kimihiko Nakano‡
*Graduate School of Engineering
the University of Tokyo, Tokyo, Japan
E-mail: xue-w@iis.u-tolyo.ac.jp
†the Institute of Industrial Science
the University of Tokyo, Tokyo, Japan
‡Interfaculty Initiative in Information Studies
the University of Tokyo, Tokyo, Japan
E-mail: knakano@iis.u-tokyo.ac.jp

***Abstract*—Dynamic driving task (DDT) fallback turns to be an essential part in level 3 or higher driving automation systems, which is responsible to either perform the DDT or achieve a minimal risk condition after encountering automated driving system (ADS) failure. As a typical ADS failure, sensor failure can prevent ADS from performing on-road driving safely, and thus a minimal risk condition can be achieved when the failed vehicle stops away from the active lane. Therefore, this paper considers a level 4 ADS-dedicated vehicle encountering front sensor failure in highway traffic. The proposed fallback approach is designed to avoid potential collision with surrounding vehicles while bringing the vehicle to a stop on the designated parking zone, thus achieve a minimal risk condition. Safety constraint is proposed based on the assumption that the failed vehicle is remarkable by surrounding vehicles, and enforced using model predictive control. As a result, simulation is conducted in Carsim/Simulink environment.**

***Keywords*—Automated vehicle, Fallback, Sensor failure, Model predictive control, Virtual lead vehicle**

I. Introduction

Driving automation at or above level 3 should have the ability to operate dynamic driving task (DDT) fallback or even become fallback-ready user when failure occurs [1]. Since human driver may be inattentive to take over the vehicle when ADS failure occurs, it can be argued that performing DDT fallback by system itself is significant in assuring the safety of driving automation. A level 4 or 5 ADS should be capable of performing DDT fallback, as well as reaching a minimal risk condition under typical ADS failures as long as basic function of the vehicle is intact.

The perception module of automated vehicle, composed of multiple sensors such as lidar, radar, camera, ultrasound, etc, is responsible for building a refined world model. Malfunction of perception module is a typical kind of ADS failure which researchers have raised concern about. Emzivat et al. consider the fallback strategy aimed at the situation when ADS loses its ability to monitor the environment as a result of system failure affecting its perception module [2]. However, their strategy is intended to mitigate potential traffic accidents instead of leading the failed vehicle to a minimal risk condition. Thus the strategy is only appropriate for limited situations. There is lack of an effective dynamic fallback approach including control process until a minimal risk condition. Therefore, the proposed fallback approach in this paper is aimed at leading a level 4 ADS-dedicated vehicle to a minimal risk condition after encountering front sensor failure in highway traffic. It is designed to remove the vehicle from active lane for a safe stop on a designated parking zone while reduce the crash risk during the fallback process.

A virtual lead vehicle method is developed in smoothing the driving task switch of adaptive cruise control system [3]. The controller generates a virtual vehicle to replace the actual lead vehicle, in order to eliminate the switching scheme between the speed and the distance control, as well as smoothly control the host vehicle to respond to the cutting in/out of the lead vehicle [4]. The proposed fallback approach implements virtual lead vehicle to replace the missing vehicle in the world of perception module, and further assumes that the virtual lead vehicle approaches the ego vehicle in a hazardous manner. Furthermore, the failed vehicle is controlled to avoid potential collision with surrounding vehicles, including virtual vehicles, before reaching a minimal risk condition using model predictive controller (MPC).

This paper is organized as follows. The proposed fallback approach is introduced in section II. Dynamic control algorithm is presented in section III, including dynamic vehicle models for longitudinal and lateral motion, and model predictive controller for realizing control targets while mitigating constraint violation. Demonstration scenarios and corresponding simulation results are shown in section IV. Finally, the research is concluded and future work is mentioned in section V.

978-1-5386-4451-5/18/$31.00 ©2018 IEEE

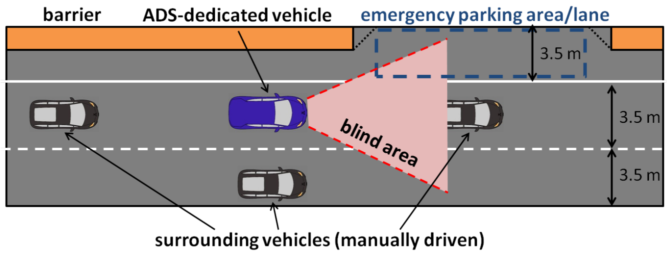

Fig. 1. Illustration of fallback scenario

II. Fallback Approach

The proposed fallback approach deals with the fallback process for an automated vehicle which is prevented from performing basic DDT on a highway by front sensor failure. It is hazardous for such a vehicle to remain on the road since ADS system cannot respond to unexpected obstacles ahead or emergent brake of its lead vehicle. Moreover, as time goes on, the failed vehicle becomes highly possible to deviate from its original lane or even have collision with highway barriers due to the missing information of road markings. The objective of the proposed fallback approach is to remove a level-4 ADS operated vehicle with front sensor failure from the active lane and park it on the designated parking zone safely and immediately.

A. Problem modeling

Sensor failure is assumed to occur on a straight section of a 2-lane, one-direction left-hand expressway featuring a hard shoulder or an emergency parking zone on its left side, whose specifications are indicated in Fig. 1. The parking zone is assumed to be unoccupied all the time. The speed limit is 50 to 100 km/h. The failed vehicle is supposed to turn on the hazard light immediately, making it remarkable for surrounding drivers.

B. Assumptions

The proposed fallback approach is based on the following assumptions:

1) Failure on sensors: Front sensors of the ego vehicle are assumed to lose its ability to collect environment information ahead, including reading road signs and perceiving the obstacles ahead. Therefore a blind area is generated in front of the ego vehicle, which is simply represented by a cone, as shown in Fig. 1. Side and rear sensors are independent of other sensors and still function well, which guarantees the ability to detect road boundary and vehicles at its sides and back. The ADS reaction time to failure is assumed to be neglectable, which means the execution of fallback starts immediately after sensor failure occurs.

2) Localization module: Localization module is mainly responsible for determining the position of ego vehicle. The localization module is assumed to work in a perfect state during the whole fallback process, and hence the vehicle retains the ability to move to the designated parking zone after failure occurs.

3) Surrounding vehicles: Surrounding vehicles indicate those which are possible to cause a collision with the ego vehicle during the fallback. The proposed fallback approach is based on the assumption that drivers in surrounding vehicles are concentrated on driving task. Surrounding vehicles are supposed to perform reasonable behaviors, including (1) keeping speed within the limit; (2) not making sharp speed variation during lane change; (3) responding to any behavior of ego vehicle after a delay of reaction time, thanks to the hazard light; (4) not occupying the designated parking zone.

C. Virtual lead vehicle

Missing vehicles due to front sensor failure are replaced with virtual lead vehicles when the fallback system is activated. The last generated world model prior to the failure of the perception module can be used to fill up the missing area in the transition stage. The virtual vehicle inherits the longitudinal position and velocity from the history data of the front vehicle that is last perceived. The virtual lead vehicle is modeled as a double integrator whose input is acceleration and outputs are the velocity and the position.

As shown in Fig. 2, to guarantee the safety of prediction on the motion of missing vehicles, the virtual vehicles are assumed to approach the ego vehicle in a hazardous manner. If the front vehicle is on the same lane with the ego vehicle, the corresponding virtual vehicle is assumed to decelerate at maximum deceleration a_m immediately, until it reaches a minimum allowable speed (50 km/h in this problem). If the front vehicle is on the different lane, the corresponding virtual vehicle is supposed to postpone the deceleration by a transient time in order to perform lane change first. The acceleration of virtual lead vehicle can be described by a step function of time $\chi_S(t)$ as follows:

$$a_{lead} = a_m \chi_S(t), \chi_S(t) = \begin{cases} 1, t \in S \\ 0, t \notin S \end{cases} \tag{1}$$

$$S = \{t | \tau_s \le t \le \tau_e, v_{fi} + \int_{\tau_s}^{\tau_e} a_m dt = v_{min}\} \tag{2}$$

where τ_s represents the time delay when lane change is necessary, τ_e represents the end time of deceleration. v_{fi} is the initial velocity of the virtual lead vehicle and v_{min} is the minimum allowable speed on the highway.

D. Fallback strategy

The objective of proposed fallback approach is to bring the failed vehicle to stop within the designated parking zone. If the failed vehicle is adjacent to a free hard shoulder, it is reasonable for the failed vehicle to leave the active lane soon after sensor failure is detected. However, in the given problem it is possible that the vehicle cannot leave the active lane immediately mainly because an emergency parking zone is provided ahead by some distance from its current position, or the vehicle is travelling on the right lane, with another active lane between the current lane and parking area.

In such situations the vehicle is required to get ready for shifting to the parking zone first. If the ego vehicle is travelling on the right lane when sensor failure is detected,

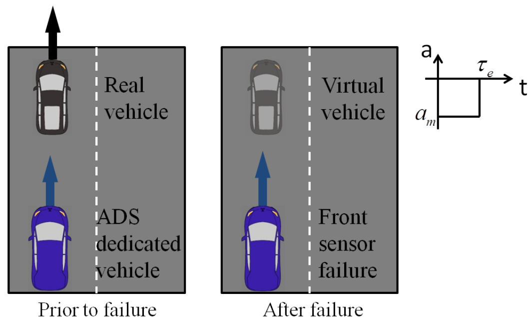

(a) The front vehicle is on the same lane as the ego vehicle is. The virtual vehicle is set to decelerate at maximum deceleration until it reaches a minimum allowable velocity

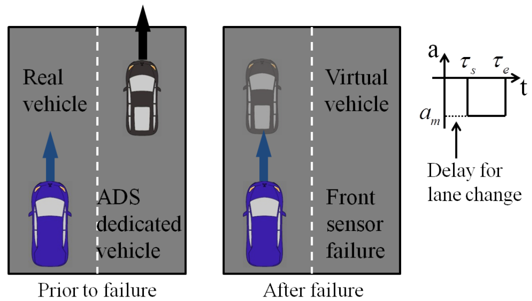

(b) The front vehicle is on the different lane. The virtual vehicle is set on the lane of the ego vehicle, while there is a time delay before deceleration because of a necessary lane change.

Fig. 2. Illustrations of virtual lead vehicle scheme

the strategy is to immediately change to the left lane as long as safe constraints between ego vehicle and surrounding vehicles are satisfied, then leave the lane to a stop when the vehicle reaches the parking zone.

E. Safety constraints

Because of acceleration and jerk restriction, vehicles with large velocity difference may run into an inevitable collision state [5] even when they do not violate the separation constraint temporarily. In other words, the remaining to collision is not enough for vehicles on the same path to adjust their velocity and thus a collision is inevitable. In this research a safety constraint based on Time to collision (TTC) [6] is constructed to prevent the occurrence of inevitable collision state during the fallback.

TTC is an indicator defined by the remaining time to collision if two vehicles keep their current speed on the collision course. Research on safe TTC criterion indicates that the determination of a safe TTC criterion depends on several factors [7] instead of a constant time. Therefore, TTC constraints in the proposed approach are developed from the assumption in section B (3) that surrounding vehicles will react to the fallback behavior of ego vehicle, which requires ego vehicle to reserve enough time for a surrounding vehicle to adjust its speed. The mathematical formula for safety constraint to be applied to the failed ego vehicle differs on the existence of rear vehicle or lead vehicle. if there is a following vehicle, the constraint is presented as:

$$\frac{\Delta L - S_{safe}}{V_r - V_e} > \tau_1 + \tau_2 + \frac{V_e - V_r}{a_m} \qquad (V_e < V_r) \tag{3}$$

where ΔL is the longitudinal distance from the head of rear vehicle to the end of front vehicle. S_{safe} is the minimum allowable distance between two vehicles on a highway. V_r and V_e represent the velocity of the rear vehicle and ego vehicle, respectively. τ_1 represents the maximum reaction time for human driver, while τ_2 represents the function time to reach the maximum deceleration a_m. a_m is usually determined by the maximum friction the road can provide and used as a negative value in calculation.

Since in this problem front vehicles cannot be detected owing to the front sensor failure, the safety constraint actually considers a virtual vehicle if there is a lead vehicle originally. The formula is similar with (3):

$$\frac{\Delta L - S_{safe}}{V_e - V_f} > \tau_1 + \tau_2 + \frac{V_e - V_f}{b_m} \qquad (V_e > V_f) \tag{4}$$

where V_f is the front vehicle velocity. τ_2 in inequation (4) represents the function time for the engine to supply a maximum acceleration represented by b_m.

III. Dynamic Control Algorithm

In the road coordinate system, the state of ego vehicle is described as $\boldsymbol{X} = [x, y, \theta, v, \dot{y}, \dot{\theta}]$, where x, y denotes the position. $v = \dot{x}$ is the longitudinal velocity and θ is the heading angle. The control input is $\boldsymbol{U} = [p, \delta]$, where p is the brake fluid pressure in the master cylinder of hydraulic brake system, and δ is the steering wheel angle. $\boldsymbol{V} = [x_i, y_i, v_i, ...]$ serves as the measured disturbance in the MPC controller, denotes the position and longitudinal velocity of surrounding vehicles (including virtual vehicles). Here i is the index of a surrounding vehicle.

A. Vehicle modeling

Longitudinal and lateral motion can be assumed decoupled when the steering angle is small [8], thus the longitudinal and lateral motion model is constructed respectively.

1) Longitudinal motion model: Longitudinal motion model takes the brake torque on front and rear wheels as input, while taking rolling resistance and aerodynamic resistance into account. The master cylinder pressure p is assumed as a direct input, which can be modified by electrical brake system, to the brake actuator. The function relating the pressure to the brake torque T_α is described as follows:

$$T_\alpha(t) = K_\alpha p(t)(\alpha \in [rear, front]) \tag{5}$$

where K_α is the gain relating master cylinder pressure with brake torque on rear and front wheel respectively. It needs to notice that this function neglects the transport delay of brake fluid.

The model ignores the slope resistance term since all the scenarios is built on a horizontal road. Moreover, no longitudinal slip is assumed for simplification. The simplified model is as follows:

$$(2T_f + 2T_r - M_r)/r_e - f_{aero} = (M + J/r_e)\dot{v} \tag{6}$$

where T_f and T_r are the brake torque on each front and rear wheel, M_r and f_{aero} are the total rolling resistance moment on wheels and aerodynamic resistance force, respectively. M and J respectively represent the total vehicle mass and the total spin inertia for wheels, and r_e is the effective radius of wheel. The rolling resistance moment is modeled as an affine function of the longitudinal velocity while aerodynamic resistance force is a quadratic function of velocity, respectively defined as follows:

$$M_r = Mgr_e(R_{rc} + R_{rv}v) \tag{7}$$

$$f_{aero} = \frac{1}{2}\rho C A v^2 \tag{8}$$

with:
g: the gravity acceleration, taking $10m/s^2$ in this work.
R_{rc}, R_{rv}: the constant and speed varying component of rolling resistance coefficients.
ρ: air mass density, choosing $1.206kg/m^3$ in this paper.
C: aerodynamic drag coefficient.
A: frontal cross-section area.

2) Lateral motion model: A 2-DOF bicycle model is used in the lateral motion control, where the lateral force on a wheel is linearized about the small slip angle. Equations of motion are shown in the road coordinate system as:

$$\begin{aligned} M\ddot{y} + \frac{2(K_f + K_r)}{v}\dot{y} + \frac{2(l_f K_f - l_r K_r)}{v}\dot{\theta} \\ - 2(K_f + K_r)\theta = 2K_f\lambda\delta \end{aligned} \tag{9}$$

$$\begin{aligned} \frac{2(l_f K_f - l_r K_r)}{v}\dot{y} + I\ddot{\theta} + \frac{2(l_f^2 K_f + l_r^2 K_r)}{v}\dot{\theta} \\ - 2(l_f K_f - l_r K_r)\theta = 2l_f K_f\lambda\delta \end{aligned} \tag{10}$$

where K_f and K_r represent the cornering stiffness of front and rear wheels, l_f, l_r represent the longitudinal distance from the gravity center to the front and rear axle. I is the yaw moment of inertia, and λ is the steering gear ratio.

B. Vehicle control method

The classic MPC controller relies on a linear model obtained by system identification. Although the vehicle is modeled by a nonlinear model, error is acceptable if the vehicle model is linearized by estimated states. In this work an adaptive model predictive controller featuring a model linearization operated on estimated states at each iteration is applied to the vehicle control. As illustrated in Fig. 3, A linear model derived from the vehicle model in section A is constructed with the help of measured outputs such as ego vehicle position collected by sensors, and unmeasurable states estimated by Extended Kalman Filter (EKF) [9]. EKF is a common used extension of Kalman Filter on nonlinear model. Then the linearized model is used to update the vehicle plant embedded in the MPC controller at each iteration. Eventually MPC transports the optimized control input to the actuator to realize an optimal control on the ego vehicle. The details of EKF are not presented in the paper due to the fully development of Kalman Filter theory.

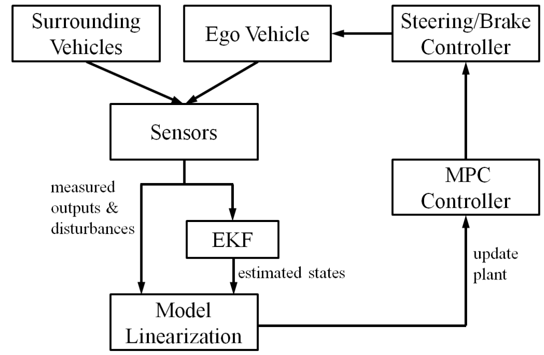

Fig. 3. Structure sketch of an adaptive MPC controller

1) Model linearization: For a nonlinear model, $\dot{\boldsymbol{X}} = F(\boldsymbol{X}, \boldsymbol{U}), \boldsymbol{Y} = G(\boldsymbol{X}, \boldsymbol{V})$, it can be linearized by a one-order Taylor series around the steady-state operating point $(\boldsymbol{X}_s, \boldsymbol{U}_s, \boldsymbol{V}_s)$ as follows:

$$\dot{\boldsymbol{X}} \approx F(\boldsymbol{X}_s, \boldsymbol{U}_s) + \nabla F(\boldsymbol{X}_s, \boldsymbol{U}_s) \begin{bmatrix} \boldsymbol{X} - \boldsymbol{X}_s \\ \boldsymbol{U} - \boldsymbol{U}_s \end{bmatrix} \tag{11}$$

$$\boldsymbol{Y} \approx G(\boldsymbol{X}_s, \boldsymbol{V}_s) + \nabla G(\boldsymbol{X}_s, \boldsymbol{V}_s) \begin{bmatrix} \boldsymbol{X} - \boldsymbol{X}_s \\ \boldsymbol{V} - \boldsymbol{V}_s \end{bmatrix} \tag{12}$$

where ∇F and ∇G is the gradient of function F and G.

The linearized approximation above can be used for MPC controller to optimize the fallback behavior.

2) MPC formulation: MPC optimizes a finite time-horizon, named prediction horizon, while only implementing the control input at the current timeslot and repeat the optimization process iteratively. The MPC problem on system input $\boldsymbol{U}$, input rate $\Delta\boldsymbol{U}$, output $\boldsymbol{Y}$ and output reference r over a prediction horizon n_p is formulated as follows:

$$\begin{aligned} \min_u J_k = & \sum_{i=k+1}^{k+n_p} (\boldsymbol{Y}_i - \boldsymbol{r}_i)^T W_{\boldsymbol{Y}} (\boldsymbol{Y}_i - \boldsymbol{r}_i) \\ & + \sum_{i=k}^{k+n_p-1} \boldsymbol{U}_i^T W_{\boldsymbol{U}} \boldsymbol{U}_i + \Delta\boldsymbol{U}_i^T W_{\Delta\boldsymbol{U}} \Delta\boldsymbol{U}_i \\ & + \rho_\varepsilon \varepsilon^2 \\ s.t. \boldsymbol{Y}_{min}(i) - \varepsilon\boldsymbol{B}_{min}(i) & \preceq \boldsymbol{Y}(k+i+1|k) \preceq \\ & \boldsymbol{Y}_{max}(i) + \varepsilon\boldsymbol{B}_{max}(i) \\ & \boldsymbol{U}_{min}(i) \preceq \boldsymbol{U}(k+i|k) \preceq \boldsymbol{U}_{max}(i) \\ & \Delta\boldsymbol{U}_{min}(i) \preceq \Delta\boldsymbol{U}(k+i|k) \preceq \Delta\boldsymbol{U}_{max}(i) \\ & i = 0, 1, ..., n_p - 1 \\ & \varepsilon \geq 0 \end{aligned} \tag{13}$$

where $W_{\boldsymbol{Y}}$, $W_{\boldsymbol{U}}$ and $W_{\Delta\boldsymbol{U}}$ denote weight matrices on output, input and input rate. ρ_ε represents the penalty on maximum constraint violation, ε. The notation $(k + i|k)$ represents the value prediction of time $k + i$ based on the available information at time k. The vector $\boldsymbol{B}_{min}$ and $\boldsymbol{B}_{max}$ are the minimum and maximum band for constraint softening. Constraints considered in the controller include road boundary, speed limit and saftey constraints in inequation $(3, 4)$.

3) Control reference: Reference for longitudinal velocity is defined as a velocity scheme with uniform deceleration a_r (set as negative) while enforcing the constraint below:

$$x - v^2/a_r < x_e \tag{14}$$

where x_e is the end position of the designated parking zone. This constraint prevents the ego vehicle from moving over the longitudinal border of the designated parking zone.

Reference for lateral motion is defined by a 3-order polynomial expression as follows:

$$r_y(t) = (y_e - y_s)\left[-2(\frac{t}{T_l})^3 + 3(\frac{t}{T_l})^2\right] + y_s \tag{15}$$

where $r_y(t)$ is the reference of lateral position. y_e and y_s respectively represents the target and starting lateral position. T_l is a default time cost on lateral shift.

IV. Simulation for Demonstration Scenarios

A. Test scenarios

Simulations of the proposed approach are conducted by Simulink and Carsim. The ego vehicle used in the simulation is typical B-class hatchback with default parameters in Carsim database. The MPC controller is built in Simulink, whose parameters are shown in Table 1. Two test scenarios are defined to evaluate the performance of the fallback approach and corresponding controller for a failed automated vehicle. The time when front sensor failure occurs is set as the initial time, and the fallback system begins to execute with no delay since ADS reaction time is ignored. The origin of coordinate is set on the initial position of the center of ego vehicle. All the vehicles in test scenarios are set as 4 m in length and 2.2 m in width.

1) Scenario I: fallback with emergency parking area: The ego vehicle is travelling on the left lane at 90 km/h when front sensor failure occurs. There is a lead vehicle on the same lane by a distance of 30 m, and a following vehicle 40 m from the ego vehicle. Both vehicles are running at 90 km/h as well. Road shoulder is not wide enough to hold a whole vehicle, but a free emergency parking area of 50 m in length and 3.5 m in width is provided 100 m before the current position of the ego vehicle in longitudinal direction.

2) Scenario II: fallback from right lane: The ego vehicle is initially travelling on the right lane at 90 km/h when front sensor failure occurs. Two vehicles are travelling on the left lane at 90 km/h, whose initial position are (-32, 3.5) and (38, 3.5). A free road shoulder lies to the left of the expressway, serving as a safe parking zone.

B. Simulation results

Simulation results of the scenarios above are given in this section. In both scenarios, the rear vehicle is set to keep its original speed until 2 seconds after the ego vehicle gives out warning, and then decelerate to 50 km/h with a constant acceleration of -2.5 m/s as response. The control input and measured output of ego vehicle are shown. Moreover, TTC spacing and corresponding constraints between ego vehicle and surrounding vehicles are illustrated to show the

TABLE I
MPC CONTROLLER PARAMETERS

Parameters	Value	Unit	Parameters	Value	Unit
T_s	0.05	s	T_l	4	s
τ_1	2.4	s	τ_2	0.9	s
a_m	-5	m/s^2	b_m	2.5	m/s^2
a_r	-2.5	m/s^2	S_{safe}	2	m
W_y	1000	-	W_v	10	-
n_p	30	-	ρ_ε	10^5	-
p_{min}	0	MPa	p_{max}	3.3	MPa
δ_{min}	-20	degree	δ_{max}	20	degree
$\Delta p_{min,max}$	±3.7	MPa/s	$\Delta\delta_{min,max}$	±15	deg/s

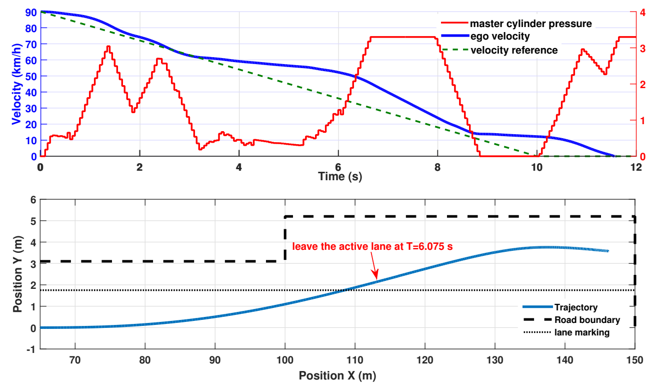

Fig. 4. Control input and output of scenario I: The ego vehicle adjusts its speed in advance to keep enough space between virtual lead vehicle and the rear vehicle. It leaves the active lane at 6.075 s for a safe stop on the emergency parking zone.

performance of the controller in guaranteeing safety.

Simulation results of scenario I are shown in Fig. 4 and Fig. 5. From the results it can be seen that the controller adjusts the vehicle speed in advance to keep enough space between both the virtual lead vehicle and the rear vehicle. The ego vehicle enters the designated parking zone at 6.075 s and then rapidly reaches a stop. The mitigation of brake input during 8∼10 s is mainly because controller needs enough lateral speed to regulate its lateral position in the parking area. MPC controller brings in a smooth speed variation with the consideration of acceleration and jerk constraints.

Figs. 6 and 7 provide the simulation results for fallback from right lane scenario. In this scenario the ego vehicle cuts into the middle of two other vehicles on the left lane since safety constraint is satisfied initially. The ego vehicle keeps its speed above the lower limit, 50 km/h, until it leaves the active lane at 7.950 s, and finally stops on the road shoulder to achieve a minimal risk condition.

Constraint violation is observed in front TTC spacing in Figs. 5 and 7, which results from 2 reasons: the virtual front vehicle is set to slow down with the maximum deceleration, so that the shrink trend of the front TTC spacing cannot be restrained and lead to a short while of constraint violation; The ego vehicle needs to reserve an enough spacing before the following vehicle. However, the TTC spacing is still higher than a critical TTC value, regarded as 1.5 s, which appears to be independent of approach speed [10]. The results indicate that the proposed fallback system is still able to avoid

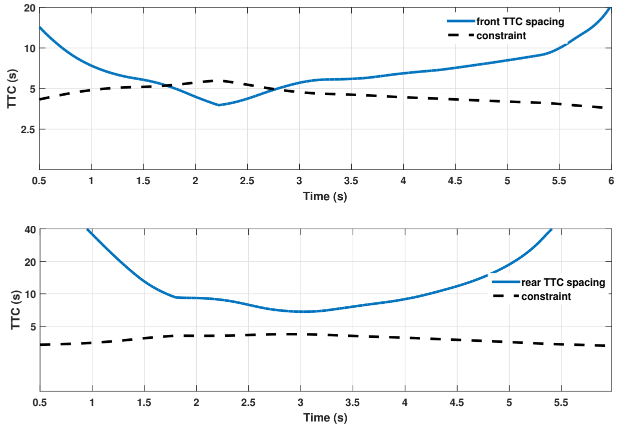

Fig. 5. TTC spacing of ego vehicle in scenario I: A slight constraint violation with front TTC spacing is caused by the close initial gap between the ego vehicle and front vehicle, and the predefined hazardous brake of the virtual lead vehicle. However, the front TTC constraint still has effect in compelling the controller to respond in advance.

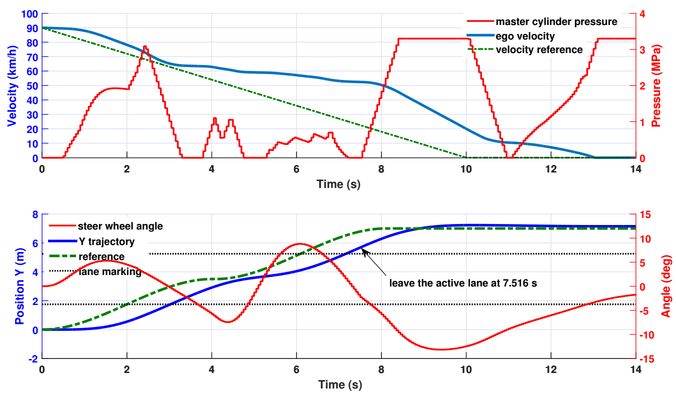

Fig. 6. Control input and output of scenario II: The ego vehicle cuts into the middle of the two other vehicles on the left lane. It leaves the active lane at 7.950 s and then comes to a stop on the free road shoulder.

a critical hazardous situation during the fallback process.

V. Conclusion

This paper proposes a dynamic fallback approach for a level-4 ADS operated vehicle encountering front sensor failure in highway traffic. The approach is designed to bring the vehicle to a safe stop on the designated parking zone. Virtual lead vehicles are generated and assumed to perform hazardous driving behaviors, which oblige the ego vehicle to actively avoid potential collision. Furthermore, a nonlinear vehicle model is employed in a MPC controller to perform optimized lateral and longitudinal control simultaneously. Through a real-time update for model linearization, the proposed MPC controller is converted to a linear quadratic optimal problem. The proposed approach is simulated in several predefined scenarios,whose feasibility to reduce crash risk and lead the failed vehicle to achieve a minimal risk condition is demonstrated.

Future work will focus on developing personalized driver model to simulate realistic reaction of human drivers in a

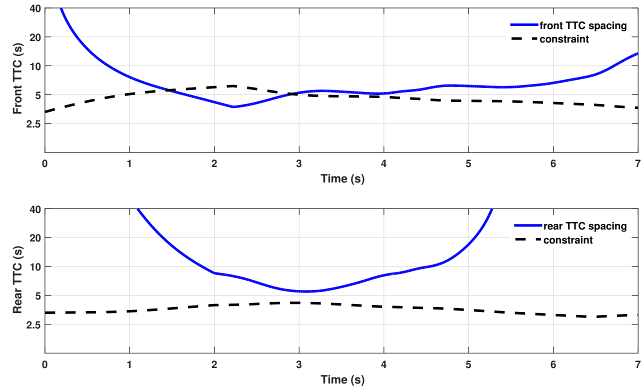

Fig. 7. TTC spacing of ego vehicle in scenario II: The constraint violation with front TTC spacing results from two reasons: there is a shorter initial space with front vehicle when cutting in; The constraint with rear vehicle restrains the sharp deceleration of ego vehicle.

fallback scenario. Further demonstration for the proposed approach by real vehicle experiments is necessary as well.

References

[1] On-Road Automated Driving (ORAD) committee. *Taxonomy and Definitions for Terms Related to Driving Automation Systems for On-Road Motor Vehicles*. SAE International, 2016

[2] Y. Emzivat, J. Ibanez-Guzman, P. Martinet, and O. H. Roux, "Dynamic driving task fallback for an automated driving system whose ability to monitor the driving environment has been compromised", in *2017 IEEE Intelligent Vehicles Symposium (IV)*, Los Angeles, CA, 2017, pp. 1841-1847.

[3] S. Kim, "Design of the adaptive cruise control systems: an optimal control approach", in Mechanical Engineering. 2012, UC Berkeley.

[4] K. Liu, J. Gong, A. Kurt, H. Chen, and U. Ozguner, "A model predictive-based approach for longitudinal control in autonomous driving with lateral interruptions", in *2017 IEEE Intelligent Vehicles Symposium (IV)*, Los Angeles, CA, 2017, pp. 359-364.

[5] R. Parthasarathi and T. Fraichard, "An inevitable collision state-checker for a car-like vehicle", in *Proceedings 2007 IEEE International Conference on Robotics and Automation*, Roma, 2007, pp. 3068-3073.

[6] J. C. Hayward, "Near miss determination through use of a scale of danger" *Highway Research Record*, vol. 384, pp. 24-34, 1972.

[7] K. Vogel, "A comparison of headway and time to collision as safety indicators", *Accident Analysis and Prevention*, 2003. 35(3), pp.427-433.

[8] K. E. Majdoub, F. Giri, H. Ouadi, L. Dugard, and F. Z. Chaoui. "Vehicle longitudinal motion modeling for nonlinear control", *Control Engineering Practice*, 2012. 20(1), pp. 69-81.

[9] H. W. Sorenson, Ed., *Kalman Filtering: Theory and Application*. Piscataway, NJ: IEEE, 1985.

[10] R. van der Horst and J. Hogema, Time-to-collision and collision avoidance systems. 1993.